Direct Imaging of Exoplanets: Science & Techniques
Proceedings IAU Colloquium No. 200, 2005
C. Aime and F. Vakili, eds.

doi:10.1017/S1743921306009987

Terrestrial Planet Finder Coronagraph Instrument Design

S. B. Shaklan, K. Balasubramanian, D. Ceperly, J. J. Green, D. J. Hoppe, O. P. Lay, P. D. Lisman and P. Z. Mouroulis

Jet Propulsion Laboratory, California Institute of Technology, 4800 Oak Grove Dr., Pasadena, CA 91009
email: stuart.b.shaklan@jpl.nasa.gov

Abstract. We describe the baseline TPF-C instrument design as of October 2005.

1. Introduction

For the past 2 years, NASA has invested substantial resources to study the design and performance of the Terrestrial Planet Finder Coronagraph (TPF-C). The work, led by the Jet Propulsion Laboratory with collaboration from Goddard Space Flight Center and several university and commercial entities, encompasses the starlight suppression system, observatory design, performance modeling, materials characterization, primary mirror studies, and a significant technology development effort including a high-contrast imaging testbed that has achieved 1e-9 contrast in a laboratory experiment (Trauger *et al.* (2005)). TPF-C papers covering the full range of these topics appear in the proceedings of the 2005 SPIE meeting (conferences 5905, 5867, and 5895) and are too numerous to list in this brief manuscript.

2. Requirements

A group of U.S.-based scientists is presently preparing the high-level science requirements. The notional requirements call for the capability to detect ∼30 terrestrial planets in the habitable zone (HZ) assuming all stars have one such planet (and likewise, ∼3 planets if the probability of occurrence of a terrestrial planet around any star is 10%).

The science requirements lead to a challenging set of performance requirements. The reflected visible/NIR light from a half-illuminated earth-like planet at 1 AU from a solar-type star is $\sim 10^{10}$ times fainter than the starlight. For a star at a distance of 10 pc, the planet appears 100 mas from the star. Studies of observing completeness (Brown (2004), Brown (2005)) and our own mission completeness studies find that to meet the science requirements for terrestrial planet detection, TPF-C should achieve the performance requirements listed in Table 1.

Table 1: TPF-C Coronagraph Contrast Error Budget Requirements

Parameter	Requirement	Comment
Static Contrast	$6\text{x}10^{-11}$	Coherent terms
Contrast Stability	$2\text{x}10^{-11}$	Thermal + Jitter
Instrument Stray Light	$1.5\text{x}10^{-11}$	Incoherent light
Inner Working Angle	4 λ/D_{long}	57 mas at λ=550 nm, D_{long} = 8 m
Outer Working Angle	48 λ/D_{short}	1.5 arcsec at λ=550 nm, D_{short}=3.5 m

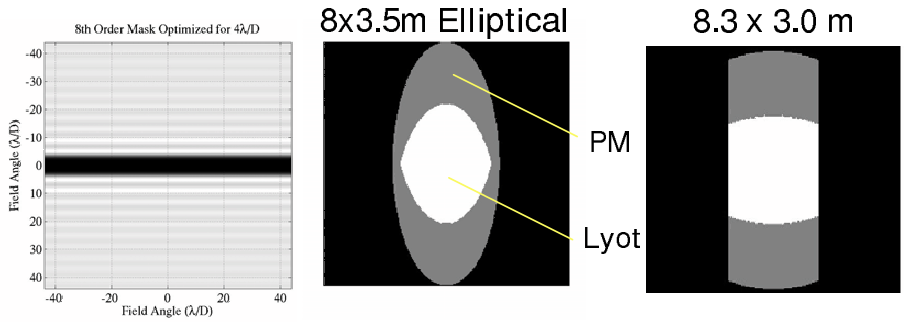

Figure 1. Left: the transmission function of the 8th-order coronagraph mask. Middle: the original 8x3.5 m elliptical paerture and Lyot stop for operation at 4λ/D. Right: the 8.3 x 3 m 'bandaid' design and corresponding Lyot stop.

"Contrast" refers to the level of light scattered by the instrument, relative the incident star light. The contrast stability is the parameter that determines the limiting signal-to-noise ratio (SNR). At a level of 2 x 10^{-11}, a planet having contrast 10^{-10} (mag = 25) can be detected with an instrument-limited SNR = 5. The inner working angle (IWA) is the closest point to the star where a planet can be detected. Extensive modeling (e.g. Green & Shaklan (2003)) has shown that for a Lyot coronagraph, it is impractical to work within 3-4 /D ($\sim$ the third Airy ring) because as one removes diffraction at smaller working angles, the Lyot aperture is reduced while aberration sensitivity increases. Our inner working angle of 4 λ/D represents a compromise between the required resolution ($\sim$60 mas), the largest aperture that can fit in an existing launch shroud, and the engineering requirements at the IWA. The outer working angle (OWA) is fundamentally limited by the number of actuators in the deformable mirror (DM). An OWA of 1.5 arcsec is achieved by spanning the short axis of the primary mirror with 96 actuators.

3. Instrument Design

3.1. *Apertures*

The aforementioned models show that monolithic apertures are far superior to segmented apertures in a high-contrast coronagraph. Segments lead to significant throughput losses at the segment edges, but more importantly relative piston motions of the segments scatters light across the coronagraph 'dark hole' and must be controlled to picometer levels. Monolithic apertures are required but are limited in their dimension by the launch vehicle shroud. Engineers at Ball Aerospace developed the concept of an elliptical aperture coronagraph (Noecker *et al.* (2003)). The long axis delivers the required resolution while the total area provides adequate sensitivity. We have recently evolved this approach from its original elliptical shape to a nearly rectangular aperture (it has the shape of a common bandage), as shown in Fig. 1

The advantages of the 'band aid' aperture are two-fold. First, in the presence of a linear occulter mask, the rectangular shape improves Lyot stop efficiency. For the case shown, it improves from 34% (elliptical) to 44% (rectangular). Second, the shape allows one to employ a so-called 'bar-code' shaped-pupil mask (Vanderbei *et al.* (2004)). These masks are straightforward to build and model, and can be made broad-band and polarization-independent.

https://doi.org/10.1017/S1743921306009987 Published online by Cambridge University Press

Table 2. Coronagraph Trades

Property	Occulter / Lyot	Shaped Pupil	PIAA	Visible Nuller
Practical IWA	3.0-3.5 λ/D	3.5-4.5 λ/D	2.0-3.0 λ/D ?	3.0-3.5 λ/D
Stop Efficiency	40-60%	25%	~100%	40-60%
Immediate Discovery Space	>70% Constrained by occulter	>70% Constrained by limited diffraction shaping	> 90% Constrained by field dependent aberrations	<25% Constrained by fringe pattern and fiber attenuation
Minimum Primary Mirror Dimensions	8x3.5 m	8x3.5 m	< 6x3.5 m	8x3.5 m
SM Despace Stability	20 nm	20 nm	1 nm ?	1 nm
Implementation Complexity	Low	Low	Moderate	High
Critical Issue	Complex errors induced at a focal plane may limit broadband utility	Interaction between high-angle diffraction and high-frequency speckles	Fabrication of optical components. Diffraction?	Implementation complexity

3.2. *Coronagraphs*

Several coronagraph forms have been considered, including band-limited Lyot coronagraphs (Kuchner & Traub (2002)), shaped pupils (Kasdin *et al.* (2003)), remapped pupils (Guyon *et al.* (2005)), a visible nulling instrument (Mennesson *et al.* (2003)), and a vortex-mask coronagraph (Palacios (2005)). Four-quadrant phase masks are not considered because their 2nd-order dependence on wave front tilt does not sufficiently suppress starlight. Vortex masks appear to have good aberration rejection and high throughput but have not been modeled to the same level of detail as band-limited masks. The baseline design includes accommodation for Lyot coronagraphs and shaped-pupils. Both can be implemented using a filter wheel approach to select different masks for different purposes (e.g. improved discovery space vs. deeper contrast over a restricted space).

Table 2 outlines the trade-offs between the various concepts. PIAA (pupil remapping) is the most promising but least mature concept. PIAA offers 100% throughput and 100% discovery space for planets outside the 2nd Airy ring. However fabrication of components and potential diffraction limitations (Vanderbei (2005)) must be explored before this approach is deemed viable. Laboratory tests in a high-dynamic range coronagraph are underway.. The baseline Lyot coronagraph is a linear 8th-order mask (Kuchner *et al.* (2005), Shaklan & Green (2005)). The 8th-order null is effective at filtering low-order aberrations that will result when the primary mirror sees thermal gradients and when the secondary mirror moves relative to the primary. Compared to a 4th-order null (e.g. the visible nuller), the 8th-order mask is 1–2 orders of magnitude less sensitive to changes in aberration content at the IWA. It also offers excellent discovery space – a planet can be detected with nearly equal efficiency beyond the IWA except for a central strip running orthogonal to the mask oscillations. The mask will likely be fabricated in HEBS glass (Trauger *et al.* (2005)) as this continuous-tone approach is the least polarization sensitive. We are currently addressing achromatization of the mask densification process. Binary mask implementations (e.g. notch-filter masks, (Kuchner & Spergel (2003)) have severe polarization and chromaticity issues (Lay *et al.* (2005)). The bar-code shaped-pupil mask shares low aberration sensitivity and large discovery space with the 8th-order mask. It has comparable throughput at the IWA but worse throughput for planets at $> \sim 6\ \lambda/D$. It is the simplest form of coronagraph to implement.

3.3. *Wave Front Control (WFC)*

Our WFC system employs two high-performance Xinetics DMs (Ealey & Trauger (2004)) arranged in a Michelson interferometer configuration. This allows independent control of

https://doi.org/10.1017/S1743921306009987 Published online by Cambridge University Press

both phase and amplitude over the dark hole, but the wave front correction has wavelength dependence that does precludes fulll correction of reflectivity and phase-induced amplitude errors over a broad spectral band. We are also considering ways to implement sequential DMs to help conjugate far-from-pupil optics. This approach may also eliminate the need for the Michelson beamsplitter and wedges which are likely to introduce additional chromatic and polarization issues. The DM format is 96 x 96 actuators on a 1 mm pitch. Thermal stabilization of the DMs is crucial – sub-Angstrom wave front stability is required during the extent of our 'set-and-forget' observing scenario (Shaklan *et al.* (2005)).

3.4. *Other Aspects*

The optical design includes an afocal cylindrical telescope that reimages the short axis of the telescope across the full width of the DM (thus forming a square image of the primary aperture on the DM). This increase the outer working angle, significantly expanding the detection space of detection of Jovian planets. The design also includes two orthogonal polarization channels. This was originally implemented for three reasons. First, the slightly different aberration content of each polarization leaked around the 4th order mask resulting in unacceptable static contrast. Second, binary masks are not simultaneously effective in both polarizations. These issues are remedied through the use of 8th order masks and by employing HEBS masks rather than binary ones. Third, the secondary channel offers full redundancy in case of DM or detector failure. We are currently considering eliminating the second channel and readdressing the redundancy issues.

Acknowledgements

The work described here has been performed at the Jet Propulsion Laboratory, California Institute of Technology, under a contract with the National Aeronautics and Space Administration.

References

Brown, R.A. 2004 *ApJ* 607, 1003
Brown, R.A. 2005 *ApJ* 624, 1010
Green, J.J., & Shaklan, S.B. 2003 *Proc. SPIE* 5170, 38
Guyon, O. *et al.* 2005 *ApJ* 622, 744
Ealey, M.A & Trauger, J.T. 2004 *Proc. SPIE* 5166, 172
Kasdin, N.J. *et al.* 2003 *ApJ* 582, 1147
Kuchner, M.J. & Traub, W.A. 2002 *ApJ* 570, 900
Kuchner, M.J. & Spergel, D.N. 2003 *ApJ* 594, 617
Kuchner, M.J. Crepp J. & Ge J. 2005 *ApJ* 628, 466
Lay, O.P., *et al.* 2005 *Proc. SPIE* 5905 (in press)
Mennesson, B. *et al.* 2003 *Proc. SPIE* 4860, 32
Noecker, N.C, Woodruff, R.A., & Burrows C. 2003 *Proc. SPIE* 4860, 72
Palacios, D. 2005 *Proc. SPIE* 5905 (in press)
Shaklan, S.B. & Green, J.J. 2005 *ApJ* 628, 474
Shaklan, S.B. *et al.* 2005 textitProc. SPIE 5905 (in press)
Trauger, J.T. *et al.* 2005 *Proc. SPIE* 5905 (in press)
Vanderbei, R.J., Kasdin, N.J, & Spergel, D.N. 2004 *ApJ* 615, 555.
Vanderbei, R.J. 2005 *ApJ* (submitted)